Electronic Research Archive

https://www.aimspress.com/journal/era

ERA, 33(1): 263–276.
DOI: 10.3934/era.2025014
Received: 17 November 2024
Revised: 02 January 2025
Accepted: 14 January 2025
Published: 22 January 2025

Research article

An energy-preserving exponential scheme with scalar auxiliary variable approach for the nonlinear Dirac equations

Hongquan Wang[1], **Yancai Liu**[2] **and Xiujun Cheng**[1,*]

[1] College of Science, Zhejiang Sci-Tech University, Hangzhou 310018, China

[2] School of Mathematics and Statistics, Henan University of Technology, Zhengzhou 450001, China

* **Correspondence:** Email: xiujuncheng@zstu.edu.cn.

Abstract: In this work, an energy-preserving scheme is proposed for the nonlinear Dirac equation by combining the exponential time differencing method with the scalar auxiliary variable (SAV) approach. First, the original equations can be transformed into the equivalent systems by utilizing the SAV technique. Then the exponential time integrator method is applied for discretizing the temporal derivative, and the standard central difference scheme is used for approximating the spatial derivative for the equivalent one. Finally, the reformulated systems, the semi-discrete spatial scheme, and the fully-discrete, linearly implicit exponential scheme are proven to be energy conserving. The numerical experiments confirm the theoretical results.

Keywords: nonlinear Dirac equation; exponential time integrator method; scalar auxiliary variable; energy conserving

1. Introduction

The Dirac equation, introduced by British physicist Paul Dirac in 1928, is a relativistic wave equation for spin-1/2 particles, bridging quantum mechanics and special relativity. Unlike the Schrödinger equation, which is non-relativistic and applies to particles moving at speeds much lower than the speed of light, the Dirac equation accounts for relativistic effects. While the Schrödinger equation describes wave functions with a single complex value, the Dirac equation uses bispinors wave functions represented as vectors of four complex components-reflecting its relativistic nature. Furthermore, the Dirac equation reduces to the Schrödinger equation in the non-relativistic limit, demonstrating its consistency with quantum mechanics in low-speed regimes. For massless particles, the Dirac equation simplifies to the Weyl equation, which describes particles like neutrinos. As such, the Dirac equation provides a more comprehensive framework for understanding the behavior of particles across various energy and velocity scales [1, 2].

A key characteristic of the Dirac equation, especially in its nonlinear form, is its ability to describe relativistic quantum systems with intrinsic spin-1/2 properties. It has profound implications in quantum field theory, where it plays a central role in the study of fermions and antimatter. The Dirac equation also appears in condensed matter physics, particularly in the study of materials like graphene and topological insulators, where low-energy excitations behave as Dirac fermions. Given its extensive applications across high-energy physics, condensed matter, and gravitational theories, significant efforts have been made to develop accurate numerical methods for solving the Dirac equation.

In this work, we focus on numerically solving the nonlinear Dirac equation in (1 + 1)-dimensions, meaning one temporal dimension and one spatial dimension, which is represented as:

$$\mathbf{i}\partial_t\Phi = \Big[-\mathbf{i}\sigma_1\partial_x + \sigma_3\Big]\Phi + \Big[V(x)I_2 - A(x)\sigma_1\Big]\Phi + F(\Phi)\Phi,\ x \in \mathbb{R},\ t > 0, \tag{1.1a}$$

$$\Phi(x,0) = \Phi_0(x),\ \lim_{|x|\to\infty}\Phi(x,t) = 0,\ x \in \mathbb{R},\ t > 0, \tag{1.1b}$$

with

$$F(\Phi) = \lambda_1(\Phi^*\sigma_3\Phi)\sigma_3 + \lambda_2|\Phi|^2 I_2,$$

where $\mathbf{i} = \sqrt{-1}$, $\lambda_1, \lambda_2 \in \mathbb{R}$,$\Phi = \Phi(x,t) = \big(\phi_1(x,t), \phi_2(x,t)\big)^\top$, $\Phi_0(x) = (\phi_{01}(x), \phi_{02}(x))^\top$ stands the spinor field with the superscript $\top$ denoting the transpose, $\phi_1, \phi_2, \phi_{01}, \phi_{02}$ are complex-valued functions, Φ^* is the conjugate transpose of Φ, $V(x)$ and $A(x)$ are the real-valued time-independent electric potential and magnetic potential, respectively, and $\sigma_k (k = 1, 3)$ denote the Pauli matrices, i.e.,

$$\sigma_1 = \begin{pmatrix} 0 & 1 \\ 1 & 0 \end{pmatrix}, \sigma_3 = \begin{pmatrix} 1 & 0 \\ 0 & -1 \end{pmatrix}.$$

The equations (1.1) possess the energy conservation law:

$$E(t) = \int_{\mathbb{R}} \Big[-\mathbf{i}\Phi^*\sigma_1\partial_x\Phi + \Phi^*\sigma_3\Phi + V(x)|\Phi|^2 - A(x)\Phi^*\sigma_1\Phi + \frac{\lambda_1}{2}(\Phi^*\sigma_3\Phi)^2 + \frac{\lambda_2}{2}|\Phi|^4\Big]dx \equiv E(0).$$

There are several efficient numerical methods available for solving the Dirac equation, such as the fourth-order compact finite difference method [3], exponential wave integrator methods for the Dirac equation with small potentials [4], finite difference time domain methods [5], and uniformly accurate (UA) schemes [6] for the Dirac equation in the nonrelativistic limit regime, and so on [7–10]. These methods are capable of solving many real-life problems, especially in the areas of fluid dynamics [11–13], biomechanics, aerodynamics, and areas wherever PDEs arise on the curved domains or domains that are challenging to mesh [14–19], even when dealing with very stiff problems [20–22]. The scalar auxiliary variable (SAV) method is an efficient approach for constructing energy-stable schemes for nonlinear systems. By reformulating nonlinear terms, it ensures energy stability while solving only decoupled linear systems with constant coefficients at each time step. This contrasts with other methods, like the fully implicit method, which require an iterative process to solve nonlinear systems. The SAV method¡¯s simplicity and reduced computational cost make it a practical and effective tool for dissipative and conservative systems in various applications [23–25]. Zhe and Shen [8] developed two SAV/CN-Hermite conservative schemes for one- and two-dimensional nonlinear Dirac equations. Yang and Xing [9] proposed a fully discrete, energy-conserving, discontinuous Galerkin method using the scalar auxiliary variable (SAV) technique for solving the Dirac equation. Additionally, several techniques have been developed for constructing higher-order linearly implicit schemes,

such as the SAV Runge–Kutta methods [26] and the relaxation Runge–Kutta methods [27]. More related work can be found in [28–32]. Moreover, the exponential integrator [33] is widely recognized for its ability to exactly integrate the linear component of a given equation, enabling it to achieve stability and efficiency, particularly for stiff differential equations, such as highly oscillatory ODEs and semidiscrete time-dependent PDEs.

In this work, we propose a linearly implicit energy-preserving scheme for solving the nonlinear Dirac equation by leveraging the exponential time differencing method in combination with the scalar auxiliary variable (SAV) approach. First, we introduce a scalar auxiliary variable to reformulate the original nonlinear Dirac equation into an equivalent system of equations. Then, the exponential time integrator is utilized to discretize the temporal derivatives, while the standard central difference method is employed to approximate the spatial derivatives. Finally, the reformulated systems, semi-discrete spatial schemes, and the fully discrete, linearly implicit exponential schemes are proven to be energy-preserving. The proposed schemes offer several advantages. One is that the schemes are linearly implicit, requiring only the solution of linear systems at each time step. The other is that the schemes ensure energy conservation for the nonlinear Dirac equation without any limitations.

The rest of the paper is organized as follows. In Section 2, the (1 + 1)-dimensional Dirac system can be rewritten as the reformulated one with the SAV approach. In Section 3, the spatial discretization semi-scheme is presented and the corresponding conservative property is given. In Section 4, the linearly implicit energy-preserving time exponential scheme is presented. In Section 5, numerical experiments are carried out to show the theoretical results.

2. Reformulation through the SAV approach

Let $\phi_1(x,t) = p_1(x,t) + \mathbf{i}q_1(x,t), \phi_2(x,t) = p_2(x,t) + \mathbf{i}q_2(x,t)$, where $p_1,\ q_1,\ p_2$, and q_2 are real functions to be solved. The system (1.1) can be written as follows:

$$\partial_t p_1 + \partial_x p_2 - q_1 - V(x)q_1 + A(x)q_2 - \lambda_1(p_1^2 + q_1^2 - p_2^2 - q_2^2)q_1 - \lambda_2(p_1^2 + q_1^2 + p_2^2 + q_2^2)q_1 = 0, \quad (2.1a)$$

$$\partial_t q_1 + \partial_x q_2 + p_1 + V(x)p_1 - A(x)p_2 + \lambda_1(p_1^2 + q_1^2 - p_2^2 - q_2^2)p_1 + \lambda_2(p_1^2 + q_1^2 + p_2^2 + q_2^2)p_1 = 0, \quad (2.1b)$$

$$\partial_t p_2 + \partial_x p_1 + q_2 - V(x)q_2 + A(x)q_1 + \lambda_1(p_1^2 + q_1^2 - p_2^2 - q_2^2)q_2 - \lambda_2(p_1^2 + q_1^2 + p_2^2 + q_2^2)q_2 = 0, \quad (2.1c)$$

$$\partial_t q_2 + \partial_x q_1 - p_2 + V(x)p_2 - A(x)p_1 - \lambda_1(p_1^2 + q_1^2 - p_2^2 - q_2^2)p_2 + \lambda_2(p_1^2 + q_1^2 + p_2^2 + q_2^2)p_2 = 0. \quad (2.1d)$$

Define $z = (p_1,\ q_1,\ p_2,\ q_2)^T$ and functional $S(z) = S_1(z) + S_2(z)$ with

$$S_1(z) = -1/2(p_1^2 + q_1^2 - p_2^2 - q_2^2) - 1/2V(x)(p_1^2 + q_1^2 + p_2^2 + q_2^2) + A(x)(p_1p_2 + q_1q_2),$$
$$S_2(z) = -1/4\lambda_1(p_1^2 + q_1^2 - p_2^2 - q_2^2)^2 - 1/4\lambda_2(p_1^2 + q_1^2 + p_2^2 + q_2^2)^2.$$

By introducing a scalar auxiliary variable $q(t) = \sqrt{\int_{\mathbb{R}} S_2(z)dx + C_0}$, , where C_0 is a positive constant to make sure that $\int_{\mathbb{R}} S_2(z)dx > -C_0$, the system (2.1) can be rewritten as

$$D\partial_t z + K\partial_x z = Nz - V(x)z + A(x)Jz + q(t)\frac{\nabla_z S_2(z)}{\sqrt{\int_{\mathbb{R}} S_2(z)dx + C_0}}, \quad (2.2a)$$

$$\frac{d}{dt}q(t) = \frac{\int_{\mathbb{R}}(\partial_t z)^\top \nabla_z S_2(z)dx}{2\sqrt{\int_{\mathbb{R}} S_2(z)dx + C_0}}, \quad (2.2b)$$

$$q(0) = \sqrt{\int_{\mathbb{R}} S_2(z(x,0))dx + C_0},\ z(x,0) = (\Re\phi_{01},\ \Im\phi_{01},\ \Re\phi_{02},\ \Im\phi_{02})^\top, \tag{2.2c}$$

where $\Re$ denotes the real part, $\Im$ denotes the imaginary part, and

$$D = \begin{pmatrix} 0 & 1 & 0 & 0 \\ -1 & 0 & 0 & 0 \\ 0 & 0 & 0 & 1 \\ 0 & 0 & -1 & 0 \end{pmatrix}, K = \begin{pmatrix} 0 & 0 & 0 & 1 \\ 0 & 0 & -1 & 0 \\ 0 & 1 & 0 & 0 \\ -1 & 0 & 0 & 0 \end{pmatrix}, N = \begin{pmatrix} -1 & 0 & 0 & 0 \\ 0 & -1 & 0 & 0 \\ 0 & 0 & 1 & 0 \\ 0 & 0 & 0 & 1 \end{pmatrix}, J = \begin{pmatrix} 0 & 0 & 1 & 0 \\ 0 & 0 & 0 & 1 \\ 1 & 0 & 0 & 0 \\ 0 & 1 & 0 & 0 \end{pmatrix}.$$

Before giving conserving energy law, we introduce a useful lemma.

Lemma 2.1. *For any L-dimensional vector $x(t)$ dependent on t and any $L \times L$ real symmetric matrix G and real skew-symmetric matrix H, it holds that*

$$\frac{d}{dt}(x(t)^\top Gx(t)) = 2(Gx(t))^\top \frac{d}{dt}x(t), \quad x(t)^\top Hx(t) = 0.$$

Proof. The proof is completed by applying basic computation. □

Theorem 2.2. *The system* (2.2) *admits the following energy conservation law:*

$$E_s(t) = \int_{\mathbb{R}} (z^\top Kz_x - 2S_1(z))\, dx - 2q(t)^2 \equiv E_s(0), \quad t \geq 0.$$

Proof. Multiplying both sides of (2.2a) on the left by $-2(\partial_t z)^\top$ and integrating over $\mathbb{R}$ respect to x, and using Lemma 2.1, one has

$$\frac{d}{dt}\int_{\mathbb{R}} \Big[z^\top Kz_x + z^\top(-N + V(x) - A(x)J)z\Big]dx - \frac{2\int_{\mathbb{R}}(\partial_t z)^\top \nabla_z S_2(z)dx}{\sqrt{\int_{\mathbb{R}} S_2(z)dx + C_0}}q(t) = 0. \tag{2.3}$$

Multiplying both sides of (2.2b) by $2q$ gives

$$\frac{d}{dt}q(t)^2 = \frac{\int_{\mathbb{R}}(\partial_t z)^\top \nabla_z S_2(z)dx}{\sqrt{\int_{\mathbb{R}} S_2(z)dx + C_0}}q(t). \tag{2.4}$$

Combining (2.3) with (2.4), the proof is complete. □

3. Energy-preserving spatial semi-discretization

Truncate the whole space problem onto an interval $[a, b]$ with zero boundary conditions and consider a finite time interval $[0, T]$. Divide $[a, b]$ into M parts and denote $h = (b-a)/M$, $\Omega_h = \{x_j = a + jh | 0 \leq j \leq M\}$. Let $X_M = \{v | v = \{v_j | 1 \leq j \leq M-1\}\}$ be a grid function space on Ω_h, and for any $u, v \in X_{4M}$, define $\delta_x u_j = (u_{j+1} - u_{j-1})/(2h)$, $\langle u, v\rangle = h\sum_{j=1}^{4M-4} u_j^\top v_j$. Before presenting the scheme of system (2.2), we introduce a circular matrix

$$B = \frac{1}{2h}\begin{pmatrix} 0 & 1 & 0 & \cdots & 0 & 0 \\ -1 & 0 & 1 & \cdots & 0 & 0 \\ 0 & -1 & 0 & \cdots & 0 & 0 \\ \vdots & \vdots & \vdots & \ddots & \vdots & \vdots \\ 0 & 0 & \cdots & \cdots & 0 & 1 \\ 0 & 0 & \cdots & \cdots & -1 & 0 \end{pmatrix}_{M-1\times M-1},$$

and define

$$\tilde{V} = \mathrm{Diag}\,(V_1, V_2, \cdots, V_{M-1}) \otimes I_4, \quad \tilde{A} = \mathrm{Diag}\,(A_1, A_2, \cdots, A_{M-1}) \otimes I_4,$$
$$\tilde{B} = B \otimes I_4, \quad \tilde{D} = I_{M-1} \otimes D, \quad \tilde{K} = I_{M-1} \otimes K, \quad \tilde{N} = I_{M-1} \otimes N, \quad \tilde{J} = I_{M-1} \otimes J,$$

with $V_j = V(x_j)$, $A_j = A(x_j)$.

By applying the second-order central difference method for spatial discretization and the trapezoidal quadrature formula in system (2.2), one obtains

$$\tilde{D}\frac{d}{dt}z_{M-1} = -\tilde{B}\tilde{K}z_{M-1} + \tilde{N}z_{M-1} - \tilde{V}z_{M-1} + \tilde{A}\tilde{J}z_{M-1} + q_{M-1}(t)\frac{\nabla_z S_2(z_{M-1})}{\sqrt{\langle S_2(z_{M-1}), \mathbf{1}\rangle + C_0}}, \tag{3.1a}$$

$$\frac{d}{dt}q_{M-1}(t) = \frac{\langle \nabla_z S_2(z_{M-1}), \frac{d}{dt}z_{M-1}\rangle}{2\sqrt{\langle S_2(z_{M-1}), \mathbf{1}\rangle + C_0}}, \tag{3.1b}$$

$$q_{M-1}(0) = \sqrt{\langle S_2(z_{M-1}(0)), \mathbf{1}\rangle + C_0}, \quad ((z_{M-1})(0))_j = z(x_j, 0), \quad 1 \le j \le M-1, \tag{3.1c}$$

where $\mathbf{1} = (1, 1, \cdots, 1)_{4(M-1)\times 1}$ and

$$z_{M-1}(t) = \Big(p_1(x_1,t), q_1(x_1,t), p_2(x_1,t), q_2(x_1,t), \cdots, p_1(x_{M-1},t), q_1(x_{M-1},t), p_2(x_{M-1},t), q_2(x_{M-1},t)\Big)^\top \in X_{4(M-1)},$$

with

$$\Big(p_1(x_0,t), q_1(x_0,t), p_2(x_0,t), q_2(x_0,t)\Big)^\top = \Big(p_1(x_M,t), q_1(x_M,t), p_2(x_M,t), q_2(x_M,t)\Big)^\top = \Big(0,0,0,0\Big)^\top.$$

Theorem 3.1. *The semi-discrete system* (3.1) *admits the following semi-discrete energy*

$$E_M(t) = \left\langle z_{M-1}, (\tilde{B}\tilde{K} - \tilde{N} + \tilde{V} - \tilde{A}\tilde{J})z_{M-1}\right\rangle - 2q_{M-1}(t)^2 \equiv E_M(0), \quad t \ge 0.$$

Proof. Taking the inner products with $-2dz_{M-1}/dt$ of (3.1a), one has

$$\begin{aligned}\left\langle \tilde{D}\frac{d}{dt}z_{M-1}, -2\frac{d}{dt}z_{M-1}\right\rangle = &\left\langle \tilde{B}\tilde{K}z_{M-1}, 2\frac{d}{dt}z_{M-1}\right\rangle + \left\langle \tilde{N}z_{M-1}, -2\frac{d}{dt}z_{M-1}\right\rangle + \left\langle \tilde{V}z_{M-1}, 2\frac{d}{dt}z_{M-1}\right\rangle \\ &+ \left\langle \tilde{A}\tilde{J}z_{M-1}, -2\frac{d}{dt}z_{M-1}\right\rangle - \frac{2\left\langle \nabla_z S_2\left(z_{M-1}\right), \frac{d}{dt}z_{M-1}\right\rangle}{\sqrt{\langle S_2\left(z_{M-1}\right), \mathbf{1}\rangle + C_0}} q_{M-1}\left(t\right).\end{aligned} \tag{3.2}$$

Based on the fact that $\tilde{B}\tilde{K}$ and $\tilde{A}\tilde{J}$ are symmetric matrices, and using Lemma 2.1, it holds that

$$\begin{aligned}&\left\langle \tilde{B}\tilde{K}z_{M-1}, 2\frac{d}{dt}z_{M-1}\right\rangle = 2h\left(\tilde{B}\tilde{K}z_{M-1}\right)^\top \frac{d}{dt}z_{M-1} = h\frac{d}{dt}\left(z_{M-1}^\top \tilde{B}\tilde{K}z_{M-1}\right) = \frac{d}{dt}\left\langle z_{M-1}, \tilde{B}\tilde{K}z_{M-1}\right\rangle, \\ &\left\langle \tilde{N}z_{M-1}, -2\frac{d}{dt}z_{M-1}\right\rangle = -\frac{d}{dt}\left\langle z_{M-1}, \tilde{N}z_{M-1}\right\rangle, \quad \left\langle \tilde{V}z_{M-1}, 2\frac{d}{dt}z_{M-1}\right\rangle = \frac{d}{dt}\left\langle z_{M-1}, \tilde{V}z_{M-1}\right\rangle, \\ &\left\langle \tilde{A}\tilde{J}z_{M-1}, -2\frac{d}{dt}z_{M-1}\right\rangle = -\frac{d}{dt}\left\langle z_{M-1}, \tilde{A}\tilde{J}z_{M-1}\right\rangle, \quad \left\langle \tilde{D}\frac{d}{dt}z_{M-1}, -2\frac{d}{dt}z_{M-1}\right\rangle = 0.\end{aligned} \tag{3.3}$$

Multiplying both sides of (3.1b) by $2q_{M-1}(t)$ gives

$$\frac{d}{dt}q_{M-1}(t)^2 = \frac{\left\langle \nabla_z S_2(z_{M-1}), \frac{d}{dt}z_{M-1}\right\rangle}{\sqrt{\langle S_2(z_{M-1}), \mathbf{1}\rangle + C_0}} q_{M-1}(t). \tag{3.4}$$

Combining (3.2)–(3.4), one gets Theorem 3.1 directly. □

4. Linearly implicit energy-preserving exponential scheme

Divide the interval $[0, T]$ into N equal parts, denote $\tau = T/N$, $t_n = n\tau$, $0 \le n \le N$, $\Omega_\tau = \{t_n | 0 \le n \le N\}$ and let $X_{MN} = \{v | v = \{v_j^n | 1 \le j \le M-1, 0 \le n \le N\}\}$ be a grid function space on $\Omega_h \times \Omega_\tau$. For any $v \in X_{MN}$, denote

$$\delta_t v_j^n = \frac{v_j^{n+1} - v_j^n}{\tau}, v_j^{n+1/2} = \frac{v_j^{n+1} + v_j^n}{2}, \hat{v}_j^{n+1/2} = \frac{3v_j^n - v_j^{n-1}}{2}.$$

Integrating the Eqs (3.1a)–(3.1b) from t_n to t_{n+1}, one has

$$z_{M-1}(t_n+\tau) = \exp(Y)z_{M-1}(t_n) + \tau\int_0^1 \exp((1-\xi)Y)\tilde{D}^{-1}f(z_{M-1}(t_n+\xi\tau), q(t_n+\xi\tau))d\xi,$$

$$q(t_n+\tau) = q(t_n) + \tau\int_0^1 \frac{\langle \nabla_z S_2(z_{M-1}(t_n+\xi\tau)), \frac{d}{dt}z\rangle}{2\sqrt{\langle S_2(z_{M-1}(t_n+\xi\tau)), \mathbf{1}\rangle + C_0}}d\xi,$$

where $Y = \tau\tilde{D}^{-1}W$, $W = -\tilde{B}\tilde{K} + \tilde{N} - \tilde{V} + \tilde{A}\tilde{J}$.

By using extrapolation method, one obtains

$$z^{n+1} = \exp(Y)z^n + \tau g(Y)\tilde{D}^{-1}f(\hat{z}^{n+1/2}, q^{n+1/2}), \quad 1 \le n \le N-1, \tag{4.1a}$$

$$q^{n+1} = q^n + \tau\frac{\langle \nabla_z S_2(\hat{z}^{n+1/2}), \delta_t z^n\rangle}{2\sqrt{\langle S_2(\hat{z}^{n+1/2}), \mathbf{1}\rangle + C_0}}, \quad 1 \le n \le N-1, \tag{4.1b}$$

$$z^1 = \exp(Y)z^0 + \tau g(Y)\tilde{D}^{-1}f(z^0, 1/2(q^0+q^1)), \tag{4.1c}$$

$$q^1 = q^0 + \tau\frac{\langle \nabla_z S_2(z^0), \delta_t z^0\rangle}{2\sqrt{\langle S_2(z^0), \mathbf{1}\rangle + C_0}}, \tag{4.1d}$$

where

$$g(Y) = \int_0^1 \exp((1-\xi)Y)d\xi, \quad f(\hat{z}^{n+1/2}, q^{n+1/2}) = \frac{\nabla_z S_2(\hat{z}^{n+1/2})}{\sqrt{\langle S_2(\hat{z}^{n+1/2}), \mathbf{1}\rangle + C_0}}q^{n+1/2}.$$

To demonstrate that the scheme (4.1) can admit a fully discrete energy, we first introduce a lemma as follows:

Lemma 4.1. *([33]) For any symmetric matrix G, skew-symmetric matrix H, and scalar $\tau \ge 0$, the matrix $\exp(\tau HG)^\top G\exp(\tau HG) - G$ is a nilpotent matrix.*

Theorem 4.2. *The linearly implicit scheme* (4.1) *admits the following discrete energy:*

$$E_h^{n+1} = E_h^n, \quad 0 \le n \le N,$$

where $E_h^n = -h(z^n)^\top Wz^n - 2(q^n)^2$.

Proof. Note that the matrix W is symmetric; assume that $\{W_\epsilon\}$ is a series of symmetric matrices satisfying $\{W_\epsilon\} \to W$ when $\epsilon \to 0$. For $1 \le n \le N-1$, let z_ϵ^n and q_ϵ^n satisfy the perturbed scheme

$$z_\epsilon^{n+1} = \exp(Y_\epsilon) z_\epsilon^n + \tau g(Y_\epsilon)\tilde{D}^{-1} f(\hat{z}_\epsilon^{n+1/2}, q_\epsilon^{n+1/2}), \tag{4.2a}$$

$$q_\epsilon^{n+1} = q_\epsilon^n + \tau \frac{\langle \nabla_z S_2(\hat{z}_\epsilon^{n+1/2}), \delta_t z_\epsilon^n \rangle}{2\sqrt{\langle S_2(\hat{z}_\epsilon^{n+1/2}), \mathbf{1}\rangle + C_0}}, \tag{4.2b}$$

where $Y_\epsilon = \tau\tilde{D}^{-1}W_\epsilon$. Denote $f_\epsilon = f(\hat{z}_\epsilon^{n+1/2}, q_\epsilon^{n+1/2})$, $\tilde{f}_\epsilon = W_\epsilon^{-1} f_\epsilon$ and

$$E_{\epsilon,h}^n = -h(z_\epsilon^n)^\top W_\epsilon z_\epsilon^n - 2(q_\epsilon^n)^2.$$

By using $\tau g(Y_\epsilon)\tilde{D}^{-1}W_\epsilon \tilde{f}_\epsilon = [\exp(Y_\epsilon) - I]\tilde{f}_\epsilon$, we can deduce from (4.2a) that

$$\begin{aligned}
(z_\epsilon^{n+1})^\top W_\epsilon z_\epsilon^{n+1} &= \Big[(z_\epsilon^n)^\top (\exp(Y_\epsilon))^\top + \tau f_\epsilon^\top (\tilde{D}^{-1})^\top g(Y_\epsilon)^\top\Big] W_\epsilon \Big[\exp(Y_\epsilon) z_\epsilon^n + \tau g(Y_\epsilon)\tilde{D}^{-1} f_\epsilon\Big] \\
&= (z_\epsilon^n)^\top (\exp(Y_\epsilon))^\top W_\epsilon \exp(Y_\epsilon) z_\epsilon^n + 2(z_\epsilon^n)^\top (\exp(Y_\epsilon))^\top W_\epsilon \Big[\exp(Y_\epsilon) - I\Big]\tilde{f}_\epsilon \\
&\quad + \tilde{f}_\epsilon^\top \Big[(\exp(Y_\epsilon))^\top - I\Big] W_\epsilon \Big[\exp(Y_\epsilon) - I\Big]\tilde{f}_\epsilon \\
&= (z_\epsilon^n)^\top (\exp(Y_\epsilon))^\top W_\epsilon \exp(Y_\epsilon) z_\epsilon^n + 2(z_\epsilon^n)^\top \Big[(\exp(Y_\epsilon))^\top W_\epsilon \exp(Y_\epsilon) - (\exp(Y_\epsilon))^\top W_\epsilon\Big]\tilde{f}_\epsilon \\
&\quad + \tilde{f}_\epsilon^\top \Big[(\exp(Y_\epsilon))^\top W_\epsilon \exp(Y_\epsilon) - (\exp(Y_\epsilon))^\top W_\epsilon - W_\epsilon \exp(Y_\epsilon) + W_\epsilon\Big]\tilde{f}_\epsilon.
\end{aligned} \tag{4.3}$$

It follows from (4.2b) that

$$\begin{aligned}
(q_\epsilon^{n+1})^2 - (q_\epsilon^n)^2 &= \frac{\langle \nabla_z S_2(\hat{z}_\epsilon^{n+1/2}), z_\epsilon^{n+1} - z_\epsilon^n\rangle}{\sqrt{\langle S_2(\hat{z}_\epsilon^{n+1/2}), \mathbf{1}\rangle + C_0}} q_\epsilon^{n+1/2} \\
&= (f_\epsilon, z_\epsilon^{n+1} - z_\epsilon^n) = h((z_\epsilon^{n+1})^\top - (z_\epsilon^n)^\top) f_\epsilon \\
&= h(z_\epsilon^n)^\top \Big[(\exp(Y_\epsilon))^\top - I\Big] f_\epsilon + \tau h f_\epsilon^\top (\tilde{D}^{-1})^\top g(Y_\epsilon)^\top f_\epsilon \\
&= h(z_\epsilon^n)^\top \Big[(\exp(Y_\epsilon))^\top W_\epsilon - W_\epsilon\Big]\tilde{f}_\epsilon + h\tilde{f}_\epsilon^\top Y_\epsilon^\top g(Y_\epsilon)^\top W_\epsilon \tilde{f}_\epsilon \\
&= h(z_\epsilon^n)^\top \Big[(\exp(Y_\epsilon))^\top W_\epsilon - W_\epsilon\Big]\tilde{f}_\epsilon + h\tilde{f}_\epsilon^\top \Big[(\exp(Y_\epsilon))^\top W_\epsilon - W_\epsilon\Big]\tilde{f}_\epsilon.
\end{aligned} \tag{4.4}$$

Combining with (4.2)–(4.4), and Lemma 4.1, we can deduce that

$$\begin{aligned}
E_{\epsilon,h}^{n+1} - E_{\epsilon,h}^n &= -h(z_\epsilon^{n+1})^\top W_\epsilon z_\epsilon^{n+1} + h(z_\epsilon^n)^\top W_\epsilon z_\epsilon^n - 2(q_\epsilon^{n+1})^2 + 2(q_\epsilon^n)^2 \\
&= -h(z_\epsilon^n)^\top \Big[(\exp(Y_\epsilon))^\top W_\epsilon \exp(Y_\epsilon) - W_\epsilon\Big] z_\epsilon^n - 2h(z_\epsilon^n)^\top \Big[(\exp(Y_\epsilon))^\top W_\epsilon \exp(Y_\epsilon) - W_\epsilon\Big]\tilde{f}_\epsilon \\
&\quad - h\tilde{f}_\epsilon^\top \Big[(\exp(Y_\epsilon))^\top W_\epsilon \exp(Y_\epsilon) - W_\epsilon\Big]\tilde{f}_\epsilon - h\tilde{f}_\epsilon^\top \Big[(\exp(Y_\epsilon))^\top W_\epsilon - W_\epsilon \exp(Y_\epsilon)\Big]\tilde{f}_\epsilon \\
&= -h(z_\epsilon^n + \tilde{f}_\epsilon)^\top \Big[(\exp(Y_\epsilon))^\top W_\epsilon \exp(Y_\epsilon) - W_\epsilon\Big]\Big(z_\epsilon^n + \tilde{f}_\epsilon\Big) - h\tilde{f}_\epsilon^\top \Big[(\exp(Y_\epsilon))^\top W_\epsilon - W_\epsilon \exp(Y_\epsilon)\Big]\tilde{f}_\epsilon = 0.
\end{aligned}$$

Accordingly, when $\epsilon \to 0$, $z_\epsilon^n \to z^n$, $q_\epsilon^n \to q^n$, and from (4.2) we can obtain

$$E_h^{n+1} = E_h^n, \quad 1 \le n \le N-1.$$

It is similar to proving that $E_h^1 = E_h^0$. Thus, the proof is complete. □

For $1 \le n \le N-1$, the solution of (4.1) can be computed as follows:
The system of (4.1) can be rewritten as

$$z^{n+1} = k^n + l^n \langle \nabla_z S_2(\hat{z}^{n+1/2}), z^{n+1} \rangle, \tag{4.5}$$

where

$$l^n = \frac{\tau g(Y) \tilde{D}^{-1} \nabla_z S_2(\hat{z}^{n+1/2})}{4\langle S_2(\hat{z}^{n+1/2}), \mathbf{1} \rangle + 4C_0},$$

$$k^n = \exp(Y) z^n + \tau g(Y) \tilde{D}^{-1} \frac{\nabla_z S_2(\hat{z}^{n+1/2})}{\sqrt{\langle S_2(\hat{z}^{n+1/2}), \mathbf{1} \rangle + C_0}} q^n - l^n \langle \nabla_z S_2(\hat{z}^{n+1/2}), z^n \rangle.$$

Taking the inner product of (4.5) with $\nabla_z S_2(\hat{z}^{n+1/2})$, one has

$$\langle \nabla_z S_2(\hat{z}^{n+1/2}), z^{n+1} \rangle = \frac{\langle \nabla_z S_2(\hat{z}^{n+1/2}), k^n \rangle}{1 - \langle \nabla_z S_2(\hat{z}^{n+1/2}), l^n \rangle}. \tag{4.6}$$

The first is to solve $\langle \nabla_z S_2(\hat{z}^{n+1/2}), z^{n+1} \rangle$ by system (4.6); the next is to get z^{n+1} by (4.5). q^{n+1} is got from (4.1) finally.

5. Numerical experiments

To support given theoretical results, some numerical tests of scheme (4.1) for model (1.1) are presented, where we choose

$$V(x) = (1-x)/(1+x^2), \quad A(x) = -(1+x)^2/(1+x^2), \quad \lambda_1 = 1, \quad \lambda_2 = 1.$$

Furthermore, we compare the proposed scheme with the following Crank–Nicolson finite difference (CNFD) scheme:

$$\mathbf{i}\delta_t \Phi_j^n = \left[-\mathbf{i}\sigma_1 \delta_x + \sigma_3 + V_j I_2 - A_j \sigma_1 + 1/2(F(\Phi_j^n) + F(\Phi_j^{n+1}))\right] \Phi_j^{n+1/2}, 1 \le j \le M-1, 0 \le n \le N-1, \tag{5.1}$$

Example 5.1. Considering the following numerical example

$$\mathbf{i}\partial_t \Phi - \left[-\mathbf{i}\sigma_1 \partial_x + \sigma_3\right]\Phi - \left[V(x) I_2 - A(x)\sigma_1\right]\Phi - F(\Phi)\Phi = f(x,t), \ x \in [0,\pi], \ t \in [0,1].$$

The exact solutions are

$$\phi_1(x,t) = \phi_2(x,t) = (t+1)\sin(x).$$

The initial conditions $\phi_{01}(x)$, $\phi_{02}(x)$, and the right-hand function $f(x,t)$ are given by the exact solutions.

To obtain numerical errors, we define the following error functions:

$$E(\tau, h) = \max_{1 \le j \le M-1} \left| \Phi(x_j, t_n) - \Phi_j^n \right|.$$

The convergence orders are calculated by $\log_2[E(\tau,h)/E(\tau/2,h)]$ in time for sufficiently small spatial steps h and $\log_2[E(\tau,h)/E(\tau,h/2)]$ in space for sufficiently small temporal steps τ. With the difference step sizes τ_0 and h_0 halved in each calculation, Example 5.1 is numerically solved by schemes (4.1) and (5.1). The global errors $E(h,\tau)$ and corresponding CPU time for scheme (4.1) are given in Tables 1 and 3, while those for the CNFD scheme are shown in Tables 2 and 4. It is observed that the scheme (4.1) works in a shorter CPU time.

Table 1. Temporal convergent order of scheme (4.1) with $h = \pi/400$.

τ	$E(h,\tau)$	Ord_τ	CPU time/s
$\tau_0 = 0.05$	4.9233e-03	*	2.1456
$\tau_0/2$	1.1010e-04	2.1608	3.3193
$\tau_0/4$	2.6982e-04	2.0287	6.5135
$\tau_0/8$	6.6567e-05	2.0191	11.5813

Table 2. Temporal convergent order of CNFD scheme with $h = \pi/400$.

τ	$E(h,\tau)$	Ord_τ	CPU time/s
$\tau_0 = 0.05$	2.9075e-03	*	15.3995
$\tau_0/2$	7.3514e-04	1.9836	21.5185
$\tau_0/4$	1.8331e-04	2.0037	41.8889
$\tau_0/8$	4.4354e-05	2.0008	70.6933

Table 3. Spatial convergent order of scheme (4.1) with $\tau = 0.002$.

h	$E(h,\tau)$	Ord_h	CPU time/s
$h_0 = \pi/10$	2.6898e-02	*	0.4215
$h_0/2$	7.3962e-03	1.8626	0.5672
$h_0/4$	1.9461e-03	1.9261	0.8877
$h_0/8$	4.8885e-03	1.9931	1.9674

Table 4. Spatial convergent order of CNFD scheme with $\tau = 0.002$.

h	$E(h,\tau)$	Ord_h	CPU time/s
$h_0 = \pi/10$	2.7102e-02	*	0.5044
$h_0/2$	7.5971e-02	1.8349	1.4662
$h_0/4$	2.0187e-03	1.9120	1.3700
$h_0/8$	5.1501e-03	1.9708	4.0939

Example 5.2. Considering the following numerical example:

$$\mathbf{i}\partial_t\Phi = \Big[-\mathbf{i}\sigma_1\partial_x + \sigma_3\Big]\Phi + \Big[V(x)I_2 - A(x)\sigma_1\Big]\Phi + F(\Phi)\Phi,\ x \in [-16,16],\ t \in [0,1].$$

The initial and boundary conditions are set to

$$\phi_1(x,0) = \exp(-x^2/2), \quad \phi_2(x,0) = \exp(-(x-1)^2/2), \quad \Phi_0^{n+1} = \Phi_M^{n+1} = 0, \quad 0 \le n \le N-1,$$

and $C_0 = 2$ in scheme (4.1).

We first test and study the convergence orders of schemes (4.1) and (5.1). We define the following error functions:

$$E_x(\tau,h)=\max_{1\le j\le M+1}\left|\Phi^n_{2j-1}(\tau,h/2)-\Phi^n_j(\tau,h)\right|,\quad E_t(\tau,h)=\max_{1\le n\le N+1}\left|\Phi^{2n-1}_j(\tau/2,h)-\Phi^n_j(\tau,h)\right|,$$

where $\Phi^n_j(\tau,h)$ is the numerical solution with time step τ and space step h. The convergence orders are calculated by $\log_2[E_t(\tau,h)/E_t(\tau/2,h)]$ in time for sufficiently small spatial steps h and $\log_2[E_x(\tau,h)/E_x(\tau,h/2)]$ in space for sufficiently small temporal steps τ. Tables 5–8 display temporal errors with $h=1/32$ and the spatial errors with $\tau=0.001$, respectively. From the tables, it is evident that the scheme (4.1) requires less CPU time and produces smaller numerical errors compared to the scheme (5.1).

Table 5. Temporal convergent order of scheme (4.1) with $h=1/32$.

τ	$E(h,\tau)$	Ord_τ	CPU time/s
$\tau_0=0.01$	6.6098e-04	*	102.5617
$\tau_0/2$	1.6724e-04	1.9827	153.6271
$\tau_0/4$	4.2065e-05	1.9912	512.7251
$\tau_0/8$	1.0547e-05	1.9957	1308.2622

Table 6. Temporal convergent order of CNFD scheme with $h=1/32$.

τ	$E(h,\tau)$	Ord_τ	CPU time/s
$\tau_0=0.01$	7.1894e-04	*	1154.6421
$\tau_0/2$	1.7984e-04	1.9991	1997.5825
$\tau_0/4$	4.4967e-05	1.9997	3464.5729
$\tau_0/8$	1.1242e-05	1.9999	7433.0148

Table 7. Spatial convergent order of scheme (4.1) with $\tau=10^{-3}$.

h	$E(h,\tau)$	Ord_h	CPU time/s
$h_0=1/4$	3.9496e-02	*	24.6294
$h_0/2$	9.6389e-03	2.0347	134.6328
$h_0/4$	2.5814e-03	1.9007	709.6157
$h_0/8$	6.5697e-04	1.9742	5905.5614

Table 8. Spatial convergent order of CNFD scheme with $\tau=10^{-3}$.

h	$E(h,\tau)$	Ord_h	CPU time/s
$h_0=1/4$	3.9655e-02	*	132.4814
$h_0/2$	1.0403e-02	1.9305	759.1494
$h_0/4$	2.7253e-03	1.9325	4718.5904
$h_0/8$	6.8641e-04	1.9893	25146.5914

The relative energy errors are calculated by $RE^n = \left|(E^n - E^0)/E^0\right|$, where E^n denotes the discrete energy at each time node. The discrete energy of both schemes and the original energy of (4.1) are shown in Figure 1. The relative energy errors are shown in Figure 2. One can see that the modified energy of scheme (4.1) differs from the original energy by a constant. The relative energy error of the scheme (4.1) is at a relatively lower value, which means the scheme can preserve the energy better.

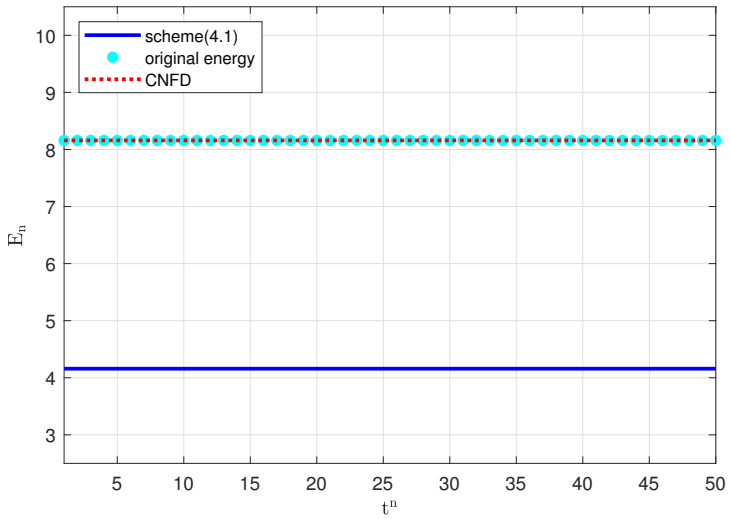

Figure 1. The discrete energy of two schemes with $\tau = 0.02$, $h = 0.1$.

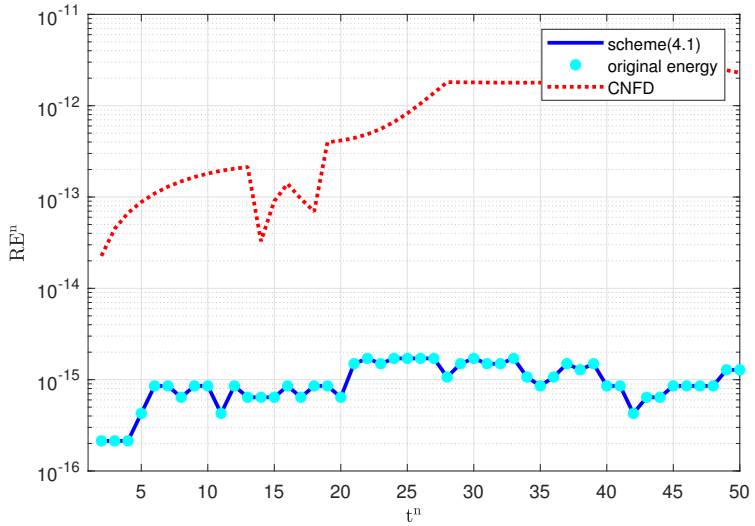

Figure 2. The energy deviation of two schemes with $\tau = 0.02$, $h = 0.1$.

Use of AI tools declaration

The authors declare they have not used Artificial Intelligence (AI) tools in the creation of this article.

Acknowledgments

This work is supported by the China Postdoctoral Science Foundation (Grant No. 2020M671087); High-Level Personal Foundation of Henan University of Technology (Grant No. 2020BS049); The corresponding author is supported by the Visiting Scholar Program of China Scholarship Council (Grant No. 202308330185).

Conflict of interest

The authors declare there are no conflicts of interest.

References

1. J. Zhang, Y. Zhang, An infinite sequence of localized semiclassical states for nonlinear Maxwell-Dirac system, *J. Geom. Anal.*, **34** (2024), 277. https://doi.org/10.1007/s12220-024-01724-4
2. N. S. Papageorgiou, J. Zhang, W. Zhang, Global existence and multiplicity of solutions for nonlinear singular eigenvalue problems, *Discrete Contin. Dyn. Syst.-S*, (2024), 1–17. https://doi.org/10.3934/dcdss.2024018
3. J. Y. Li, T. C. Wang, Optimal point-wise error estimate of two conservative fourth-order compact finite difference schemes for the nonlinear Dirac equation, *Appl. Numer. Math.*, **162** (2021), 150–170. https://doi.org/10.1016/j.apnum.2020.12.010
4. Y. Feng, Z. G. Xu, J. Yin, Uniform error bounds of exponential wave integrator methods for the long-time dynamics of the Dirac equation with small potentials, *Appl. Numer. Math.*, **172** (2022), 50–66. https://doi.org/10.1016/j.apnum.2021.09.018
5. W. Z. Bao, Y. Y. Cai, X. W. Jia, Q. L. Tang, Numerical methods and comparison for the Dirac equation in the nonrelativistic limit regime, *J. Sci. Comput.*, **71** (2017), 1094–1134. https://doi.org/10.1007/s10915-016-0333-3
6. M. Lemou, F. Méhats, X. F. Zhao, Uniformly accurate numerical schemes for the nonlinear Dirac equation in the nonrelativistic limit regime, *Commun. Math. Sci.*, **15** (2017), 1107–1128. https://doi.org/10.4310/CMS.2017.v15.n4.a10
7. K. Schratz, Y. Wang, X. F. Zhao, Low-regularity integrators for nonlinear Dirac equations, *Math.Comput.*, **90** (2021), 189–214. https://doi.org/10.1090/mcom/3557
8. Y. Zhe, J. Shen, Efficient SAV-Hermite methods for the nonlinear Dirac equation, *Discrete Contin. Dyn. Syst.-Ser. B*, **28** (2023), 3428–3452. https://doi.org/10.3934/dcdsb.2022225
9. R. Yang, Y. Xing, Energy conserving discontinuous Galerkin method with scalar auxiliary variable technique for the nonlinear Dirac equation, *J. Comput. Phys.*, **463** (2022), 111278. https://doi.org/10.1016/j.jcp.2022.111278
10. F. Fillion-Gourdeau, E. Lorin, A. D. Bandrauk, Numerical solution of the time-dependent Dirac equation in coordinate space without fermion-doubling, *Comput. Phys. Commun.*, **183** (2012), 1403–1415. https://doi.org/10.1016/j.cpc.2012.02.012

11. X. H. Yang, W. L. Qiu, H. X. Zhang, L. Tang, An efficient alternating direction implicit finite difference scheme for the three-dimensional time-fractional telegraph equation, *Comput. Math. Appl.*, **102** (2021), 233–247. https://doi.org/10.1016/j.camwa.2021.10.021
12. Z. Y. Chen, H. X. Zhang, H. Chen, ADI compact difference scheme for the two-dimensional integro-differential equation with two fractional Riemann-Liouville integral kernels, *Fractal Fractional*, **8** (2024), 707. https://doi.org/10.3390/fractalfract8120707
13. H. X. Zhang, X. H. Yang, Y. L. Liu, Y. Liu, An extrapolated CN-WSGD OSC method for a nonlinear time fractional reaction-diffusion equation, *Appl. Numer. Math.*, **157** (2020), 619–633. https://doi.org/10.1016/j.apnum.2020.07.017
14. X. H. Yang, Z. M. Zhang, Analysis of a new NFV scheme preserving DMP for two-dimensional sub-diffusion equation on distorted meshes, *J. Sci. Comput.*, **99** (2024), 80. https://doi.org/10.1007/s10915-024-02511-7
15. X. H. Yang, H. X. Zhang, Q. Zhang, G. W. Yuan, Simple positivity preserving nonlinear finite volume scheme for subdiffusion equations on general non-conforming distorted meshes, *Nonlinear Dyn.*, **108** (2022), 3859–3886. https://doi.org/10.1007/s11071-022-07399-2
16. C. J. Li, H. X. Zhang, X. H. Yang, A new linearized ADI compact difference method on graded meshes for a nonlinear 2D and 3D PIDE with a WSK, *Comput. Math. Appl.*, **176** (2024), 349–370. https://doi.org/10.1016/j.camwa.2024.11.006
17. Y. Shi, X. H. Yang, Z. M. Zhang, Construction of a new time-space two-grid method and its solution for the generalized Burgers' equation, *Appl. Math. Lett.*, **158** (2024), 109244. https://doi.org/10.1016/j.aml.2024.109244
18. X. H. Yang, W. Wang, Z. Y. Zhou, H. X. Zhang, An efficient compact difference method for the fourth-order nonlocal subdiffusion problem, *Taiwan. J. Math.*, **1** (2024), 1–32. https://doi.org/10.11650/tjm/240906
19. X. H. Yang, W. L. Qiu, H. F. Chen, H. X. Zhang, Second-order BDF ADI Galerkin finite element method for the evolutionary equation with a nonlocal term in three-dimensional space, *Appl. Numer. Math.*, **172** (2022), 497–513. https://doi.org/10.1016/j.apnum.2021.11.004
20. X. H. Yang, Z. M. Zhang, Superconvergence analysis of a robust orthogonal Gauss collocation method for 2D fourth-order subdiffusion equations, *J. Sci. Comput.*, **100** (2024), 62. https://doi.org/10.1007/s10915-024-02616-z
21. H. X. Zhang, X. H. Yang, D. Xu, Unconditional convergence of linearized orthogonal spline collocation algorithm for semilinear subdiffusion equation with nonsmooth solution, *Numer. Methods Partial Differ. Equations*, **37** (2021), 1361–1373. https://doi.org/10.1002/num.22583
22. X. H. Yang, H. X. Zhang, The uniform l^1 long-time behavior of time discretization for time-fractional partial differential equations with nonsmooth data, *Appl. Math. Lett.*, **124** (2022), 107644. https://doi.org/10.1016/j.aml.2021.107644
23. D. F. Li, X. X. Li, Relaxation exponential Rosenbrock-type methods for oscillatory Hamiltonian systems, *SIAM J. Sci. Comput.*, **45** (2023), A2886–A2911. https://doi.org/10.1137/22M1511345

24. D. F. Li, X. X. Li, J. Yang, Relaxation exponential Runge-Kutta methods and their applications to semilinear dissipative/conservative systems, *Commun. Comput. Phys.*, **36** (2024), 908–942. https://doi.org/10.4208/cicp.OA-2023-0241

25. D. F. Li, W. W. Sun, Linearly implicit and high-order energy-conserving schemes for nonlinear wave equations, *J. Sci. Comput.*, **83** (2020), 1–17. https://doi.org/10.1007/s10915-020-01245-6

26. G. Akrivis, B. Y. Li, D. F. Li, Energy-decaying extrapolated RK–SAV methods for the Allen–Cahn and Cahn–Hilliard equations, *SIAM J. Sci. Comput.*, **41** (2019), A3703–A3727. https://doi.org/10.1137/19M1264412

27. Y. R. Zhang, J. Shen, A generalized SAV approach with relaxation for dissipative systems, *J. Comput. Phys.*, **464** (2022), 111311. https://doi.org/10.1016/j.jcp.2022.111311

28. J. Xu, S. H. Shao, H. Z. Tang, Numerical methods for nonlinear Dirac equation, *J. Comput. Phys.*, **245** (2013), 131–149. https://doi.org/10.1016/j.jcp.2013.03.031

29. Y. Y. Fu, D. D. Hu, G. G. Zhang, Arbitrary high-order exponential integrators conservative schemes for the nonlinear Gross-Pitaevskii equation, *Comput. Math. Appl.*, **121** (2022), 102–114. https://doi.org/10.1016/j.camwa.2022.07.004

30. S. C. Li, X. G. Li, High-order compact methods for the nonlinear Dirac equation, *Comput. Appl. Math.*, **37** (2018), 6483–6498. https://doi.org/10.1007/s40314-018-0705-4

31. W. Z. Bao, J. Yin, A fourth-order compact time-splitting Fourier pseudospectral method for the Dirac equation, *Res. Math. Sci.*, **6** (2019), 1–35. https://doi.org/10.1007/s40687-018-0173-x

32. S. C. Li, X. G. Li, High-order conservative schemes for the nonlinear Dirac equation, *Int. J. Comput. Math.*, **97** (2020), 2355–2374. https://doi.org/10.1080/00207160.2019.1698735

33. C. L. Jiang, Y. S. Wang, W. J. Cai, A linearly implicit energy-preserving exponential integrator for the nonlinear Klein-Gordon equation, *J. Comput. Phys.*, **419** (2020), 109690. https://doi.org/10.1016/j.jcp.2020.109690

AIMS Press